Cancer Management and Research

Elevate Series

Open Access Full Text Article

ORIGINAL RESEARCH

Evaluation of Drug Effectiveness and Controlled Release Profiles of Clay Minerals Loaded with Anti-Carcinogenic Agent as a Drug Delivery System on Leukemia

Mustafa Duran[1], Elif Kaga[2]

[1]Afyonkarahisar Health Sciences University Faculty of Medicine, Department of Internal Medicine, Hematology, Afyonkarahisar, Türkiye; [2]Afyonkarahisar Health Sciences University Department of Medical Services and Techniques, Afyonkarahisar, Türkiye

Correspondence: Mustafa Duran, Afyonkarahisar Health Sciences University Faculty of Medicine, Afyonkarahisar, 03030, Türkiye, Tel +905059139577, Email mistik07@hotmail.com

Objective: Myeloid leukemia is a stem cell disease with high mortality due to the challenges of high-dose treatments and side effects. Innovative nanoparticle drug delivery systems are being explored to enhance efficacy and tissue-targeted therapy. This study investigates the potential of Bentonite (BNT)-based nanoparticles (NPs) as drug carriers for azacitidine (AZA) in treating THP-1 and K562 myeloid leukemia (AML) cell lines, aiming to improve drug stability, bioavailability, and therapeutic efficacy while ensuring controlled release.

Material and Method: Bentonite clay morphology was analyzed using Scanning Electron Microscopes. The BNT-AZA combination was tested in THP-1 and K562 cell cultures via in vitro proliferation tests, CCK-8 assays, and drug release tests with dialysis membranes. Apoptosis and internalization were evaluated using Annexin V-FITC and fluorescence methods, respectively.

Results: The BNT-AZA exhibited controlled release over 8 hours, with 50% released within 2 hours, 90% by the 4th hour, and prolonged release beyond 8 hours. This profile reduces side effects while increasing efficacy in target cells. Bentonite demonstrated significant drug-loading capacity, controlled release, and tumor-targeting capabilities. At concentrations of 10, 25, 50, and 100 µg/mL, BNT showed dose-dependent antiproliferative effects, maintaining low cytotoxicity at lower concentrations. The combination of azacytidine and bentonite exhibited a synergistic effect in inhibiting cell proliferation, with significant decreases in cell viability in the 1 µM azacytidine + 10 µg/mL bentonite, 5 µM azacytidine + 10 µg/mL bentonite, and 10 µM azacytidine + 10 µg/mL bentonite groups compared to the controls. The combination of 1 µM AZA with 10 µg/mL BNT achieved similar efficacy to 10 µM AZA alone, suggesting a potential for dose reduction and improved safety.

Conclusion: BNT nanoparticles are promising carriers for AZA, enhancing targeted delivery, reducing side effects, and potentially lowering the required dose for leukemia treatment. These findings support further investigation into the clinical application of BNT-AZA in hematologic cancers.

Keywords: Azacytidine, Bentonite, Controlled release, Cytotoxicity, Leukemia, Drug carriers

Introduction

Minerals such as Bentonite (BNT), Montmorillonite, and Kaolinite have been used for years in pharmaceutical formulations. BNT, a type of mineral, is primarily composed of 2:1 type of fillosilicates, whereas Montmorillonite (MTT) is a soft plastic substance formed from a member of the smectite family of minerals. MTT has a structural composition of aluminosilicate, with an octahedral layer consisting of Al(OH)6 octahedrons and SiO4 tetrahedrons.[1] The structure of anyon and its ease of adsorption onto alumina-silicate surfaces, as well as its larger surface area, make it advantageous for cation- anion adsorption and hydrogen binding. The cation- anion load and density of clay minerals play a significant role in the adsorption and binding processes of therapeutic agents because of their electrostatic interactions.[2,3] Nanoparticles (NP) have advanced to such an extent that they can now support certain characteristics, owing to their versatile usage. NP clay for example, come in various forms such as flat, film, or tube-like structures, and

Received: 23 August 2024
Accepted: 3 December 2024
Published: 11 December 2024

have sizes ranging from 1 to 200 mm. It is also known that the ideal size for use as a nanocarrier in drug delivery is up to 200 nm.[4] Increasing the clay lumen diameter from 10–15 nm to 30–40 nm increases the carrying capacity by 30–40%. The negative charge of the NP clay is often associated with the wide area of a specific surface, indicating a significant potential for NP clay extended binding to positively charged drugs.[5] When examining the broader context of NP based drug delivery systems, contradictions and interesting facts arise. For instance, it has been demonstrated that nanoparticles can improve the administration of anticancer medications, safeguard against enzymatic degradation, and enable targeted and/or regulated release.

The use of clay NP is not limited to drug delivery alone but also promotes an anti-proliferative effect, encourages cell-cell and cell-matrix adhesion between cancer cells, and prevents the formation of metastases in cancer cells. In particular, oral administration of drugs with emetic problems provides a therapeutic route for gastric and intestinal absorption and distribution, which is advantageous for clay NP. The solubility and biocompatibility of the drug are increased by the clay, which controls drug release, increases its durability, and protects the drug from harsh environments such as stomach acids. There is a passive targeting system with physical and chemical properties that promotes the release of NPs in tumour tissue owing to the reduction of lymphatic drainage and the increase in pH in the tumour microenvironment.[6–8] The affinity of certain receptors (such as EGFR, transferrin, and folate receptors) on the surface of tumour cells allows them to specifically target and actively engage with these receptors, leading to selective interactions with tumour cells only.[9–11] The development and design of drug carriers aimed at targeted release, controlled emission, entrapment within cells, and subsequent release into the surrounding environment have been based on certain characteristics such as those described above.[12,13] However, the number of studies conducted in this manner is insufficient. Acute myeloid leukemia (AML) is a form of leukaemia that originates from immature myeloid cells and presents aggressive symptoms. In elderly AML patients who are not suitable for intensive chemotherapy treatment, such as the 7+3 regimen, the low rates of complete remission and median survival with monotherapy using azacytidine (AZA).[14] Increasing the effectiveness of AZA in treatment will increase the chances of treatment in the older patient group and it is possible to obtain lower mortality and higher remission rates. There is a need for treatment methods to be developed for this purpose. Oral forms of HMAs, which are particularly preferred in elderly AML patients, have similar efficacy, side effects, and safety profiles as injectable forms.[15]

Research has focused on creating clay-based drug carriers with features such as prolonged circulation, controlled absorption, binding to target cells, accumulation within cells, and release.[12,13] The goal is to develop drug carrier systems that can enhance the efficacy of current treatments, extend life expectancy, improve disease-free survival and complete response rates, and minimise adverse effects. In this study, we aimed to evaluate the drug release and therapeutic potential of the AZA-BNT combination in in vitro cell cultures, with the intention of enhancing the therapeutic effectiveness of the oral form of AZA. We examined the cytotoxicity and release profile results to achieve this aim.

Material and Methods

Materials

In our study, we used BNT clay with the molecular structure OO=[Si]=OO=[Si]=OO=[Si]=OO=[Si]=OO=[Al]O[Al]=O, which primarily consists of the smectite group of clay minerals, specifically montmorillonite. BNT clay was supplied by Sigma-Aldrich. We also used AZA, which has the formula structure of 5-Azacytidine, 4-Amino-1-(β-D-ribofuranosyl)-1,3,5-triazin-2(1H)-one, and was supplied by Sigma-Aldrich. Additionally, we utilized Ladakamycin in our study, which was also supplied by Sigma-Aldrich.

Scanning Electron Microscope (SEM)

We employed the LEO-1430 VP model SEM device located at Afyon Kocatepe University, Technology Application and Research Center to examine the morphological structures of the clay minerals used in the study and to determine their diameters. Prior to the SEM analysis of the clay mineral, we coated it with gold using a Bal-Tec SCD005 Sputter Coater gold-coating device at a current of 100 mA for 20s. This coating process was performed to enhance surface conductivity

and obtain high-resolution images. After the coating process, we conducted morphological analysis of the tissue scaffolds at a voltage of 20 kV.

Drug Release Test

In the first stage of the study, a drug-loading process was conducted on BNT minerals for drug release testing. To this end, a 2 mL solution containing 10 µM AZA and 10 µg/mL BNT was prepared. The solution was then homogenized using an ultrasonic homogenizer (Bandelin 4050) for 20 min. In the second stage, the drug release test was performed using 2 mL of a solution containing AZA-loaded clay minerals, which were placed in a dialysis membrane. The dialysis membrane was then placed in 5 mL of PBS and the mixture was incubated at 37 °C in a shaking incubator at pH 7.4. Samples were taken at predetermined intervals (data points: 1 min, 5 min, 10 min, 20 min, 30 min, 40 min, 60 min, 90 min, 150 min, 240 min, 300 min, 360 min, 480 min) and the optical density at 240 nm was measured using a spectrophotometer. The resulting data were recorded and analyzed.

In Vitro Cell Culture Tests

Cell Lines

The K562 cell line, obtained from Sigma-Aldrich, comprised cells derived from a 53-year-old female patient with chronic myeloid leukaemia in a terminal blast crisis. Similarly, the THP-1 cell line, also obtained from Sigma-Aldrich, is comprised of cells derived from a patient diagnosed with acute monocytic leukaemia. In this study, both THP-1 and K-562 cell lines were cultured in medium supplemented with 10% FBS, 100 U/mL penicillin, and 100 mg/mL streptomycin. The cells were incubated at 37 °C with 5% CO2.

Cell Proliferation Assay

An in vitro cell proliferation assay was performed using a CCK-8 kit. For each concentration, the cells (5×10^3) were seeded in 96-well plates in triplicate. Following overnight incubation, the medium of adherent cells was replaced with media containing BNT, AZA, or BNT+AZA at increasing concentrations (n=4). Control cells were incubated with supplemented medium. After 48 h of incubation, 10 µL of CCK-8 solution (10% concentration) was added to each well to assess cell viability, and absorbance values were measured at 450 nm using a plate reader after a four-hour incubation period.

Internalization Test

The internalisation of BNT minerals by cells was assessed through time-dependent cell internalisation analyses using fluorescence methods with flow cytometry. Doxorubin was employed as a standard fluorescent agent. Cancer cells were seeded at a density of 5×10^4 cells/well. Prepared free Dox and DOX-loaded BNT solutions (10 µM in 1 mL medium) were applied to the cells, and samples with 30 min, 4 h, and 24 h incubation times were prepared (n=3). Following incubation, the cells were washed twice with 1x PBS. Subsequently, fixation was performed with 4% PFA, and the cells were treated with 0.25% Triton-X100 for 20 min. Images were captured in the FITC channel using Beckman DxFLEX after incubation. Image analyses were performed using the CytExpert software.

Apoptosis Test

The apoptosis assay was performed according to the protocol provided by the Annexin V-FITC Kit (Beckman Coulter Life Sciences, Brea, CA, USA). Prior to analysis, cells were seeded at a density of 5×10^5 cells/well and incubated for 24 h under conditions conducive to cell adhesion. Following this, AZA, BNT+AZA, and BNT solutions were applied to the cells, and the cells were incubated for an additional 48 h under culture conditions (n=3). Subsequently, the control groups and treated cells were trypsinised, collected, and centrifuged at 200 × G for 5 min. Following centrifugation, 100 µL annexin binding buffer was added to each group. Subsequently, 1 µL of annexin V-FITC antibody and 5 µL of PI solution were added to the mixture, and the cells were incubated in the dark for 20 min. After incubation, 500 µL of annexin buffer was added to each sample, and flow cytometric analyses were performed using a Backman DxFlEX Flow Cytometer (USA). Data analyses were performed using CytExpert Analysis Software.

Western Blot Analysis

The interaction between drug-loaded BNT and BNT proteins in cancer cells was examined using Ki-67 protein expression analysis. Prior to the experiment, cells (5×10^5) were seeded in six-well plates and maintained under cell culture conditions for 24 h. The following day, the cell culture solution was replaced with medium containing BNT, AZA, and BNT+AZA solutions. The cells were then incubated for 48 h After incubation, the cells were collected for each sample and incubated in lysis buffer containing 0.1% SDS, 1% NP-40, 50 mm HEPES (pH 7.4), 2 mm EDTA, 100 mm NaCl, 5 mm sodium orthovanadate, 40 µM p-nitrophenyl phosphate, and 1% protease inhibitor mixture on ice for 15 min. The samples were then centrifuged at 16000 g for 15 min, the supernatant was collected, and protein concentrations were measured. Equal protein concentrations were adjusted for each sample to be loaded onto the gels. The proteins were then separated based on their molecular weights using a 12% SDS-PAGE gel and blotting was performed. During blotting, proteins were transferred onto a nitrocellulose membrane. Blocking was performed with a blocking buffer composed of 0.05% Tween-20 in PBS for 1 h. Following blocking, the membrane was incubated with the primary antibody for 1 h and with peroxidase-conjugated secondary antibodies for 1 h, following washing procedures. Finally, bands were visualised on a membrane using chemiluminescence (ECL) solution.

Statistical Analysis

Data analysis was performed using Ordinary One-way ANOVA test by the GraphPad Prism 8.0 software. *P < 0.05, ¥P < 0.05, αP< 0.05, *P<0.05, **P < 0.001 compared to the control group.

Results

Microscopic Characterisation of Bentonite Using SEM

In Figure 1, the morphological and dimensional features of BNT minerals were examined using a scanning electron microscope. The SEM images reveal the presence of BNT molecules with an average size ranging between 100 and 1000 nm.

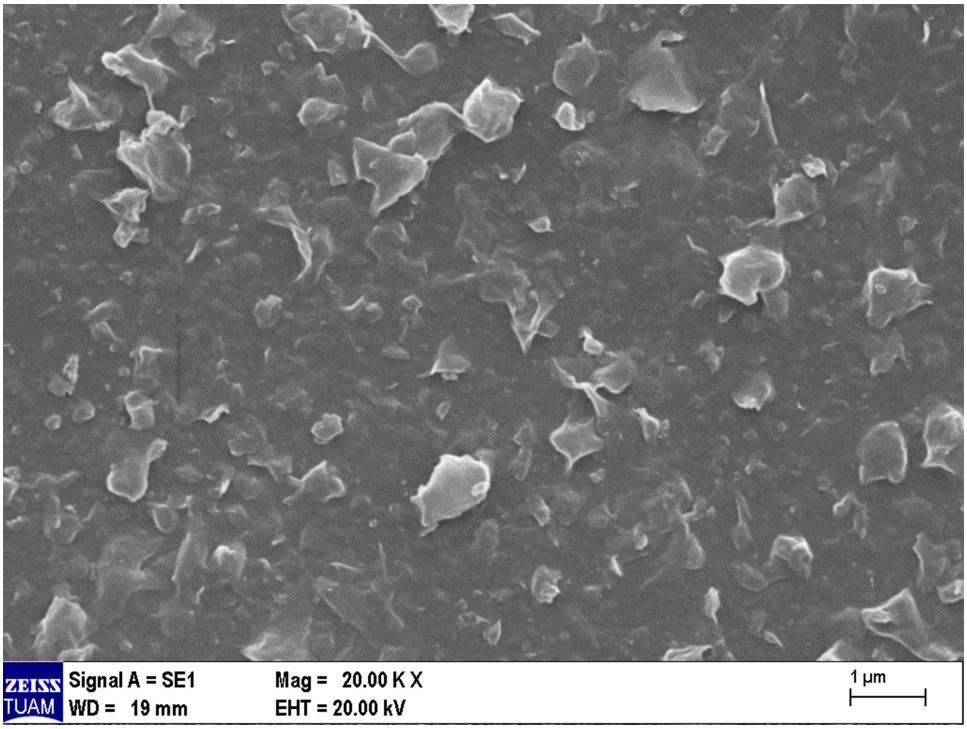

Figure 1 SEM images of bentonite mineral.

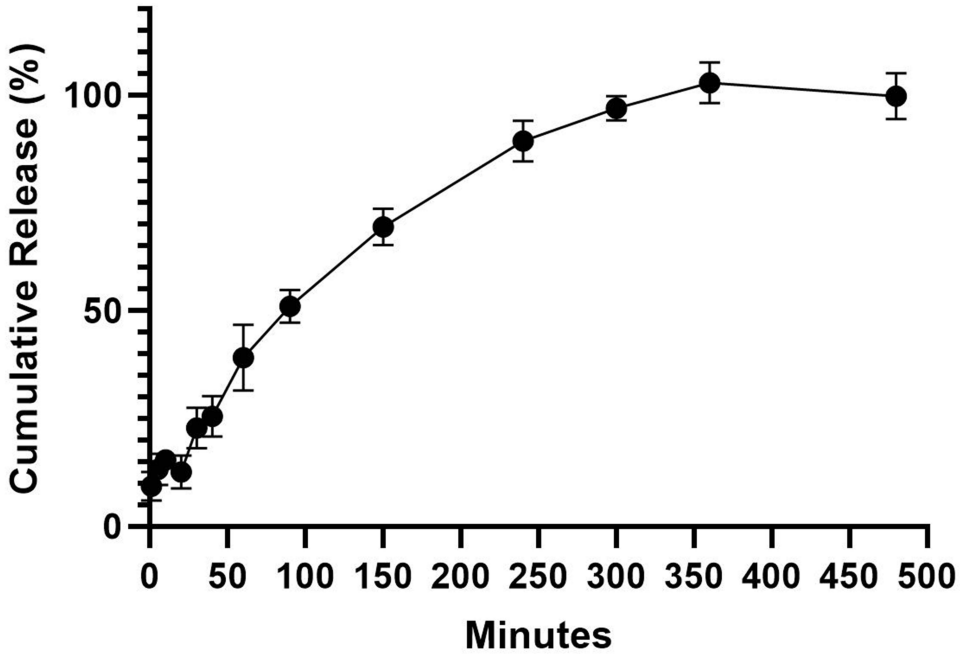

Figure 2 Bentonite mineral drug release test. Release profile of azacitidine-loaded bentonite mineral in PBS (pH 7.4). Data points: 1 min, 5 min, 10 min, 20 min, 30 min, 40 min, 60 min, 90 min, 150 min, 240 min, 300 min, 360 min, 480 min.

In vitro Drug Release Study

The drug release profile was assessed using a dialysis membrane. A specified volume of AZA-loaded BNT solution (2 mL) was placed within the dialysis membrane and at various time points (data points: 1 min, 5 min, 10 min, 20 min, 30 min, 40 min, 60 min, 90 min, 150 min, 240 min, 300 min, 360 min, 480 min), and the absorbance values were measured using a spectrophotometry at 240 nm from samples withdrawn from the exterior of the dialysis membrane. As depicted in Figure 2, the AZA-loaded BNT demonstrated controlled drug release, releasing all the drug into the solution within an 8-hour period.

Cell Culture Tests

Cell Proliferation Test

In the aforementioned investigation, human leukaemia cell lines, specifically THP-1 and K-562, were used to assess the toxic effects of BNT minerals. Prior to application onto the cells, BNT mineral was homogenised via a sonic homogeniser for 20 min and subsequently diluted to specific concentrations (0.25 µg/mL, 0.5, 1, 2.5, 5, 10, 25, 50, and 100 µg/mL) for application to the cells. The cells were incubated under standard cell culture conditions for 48 h. The control group was incubated with a solution containing only medium.

According to the dose-dependent proliferation test results depicted in Figure 3 for THP-1 cells, no toxic effect was observed with regard to the viability value in the 0.25 µg/mL, 0.5, 1, 2.5, and 5 µg/mL BNT-applied groups. However, a statistically significant decrease was observed in the 10 µg/mL, 25 µg/mL, 50 µg/mL, and 100 µg/mL BNT-treated groups compared to that in the control group. These findings indicated that BNT exhibited a significant antiproliferative effect on THP-1 cells within the specified groups.

BNT displayed a dose-dependent proliferation effect on K562 cells, as demonstrated in Figure 4, which showed no toxic effect on cell viability at concentrations of 0.25 µg/mL, 0.5, 1, 2.5, and 5 µg/mL. However, a statistically significant decrease in cell viability was observed in the groups treated with 10, 25, 50, and 100 µg/mL BNT mineral, indicating a significant antiproliferative effect on K562 cells at these concentrations.

In the second stage of the proliferation assay, BNT and the anti-cancer drug AZA were administered separately and in combination to assess their effects on the growth of THP-1 and K562 cells. The cells were divided into groups based on

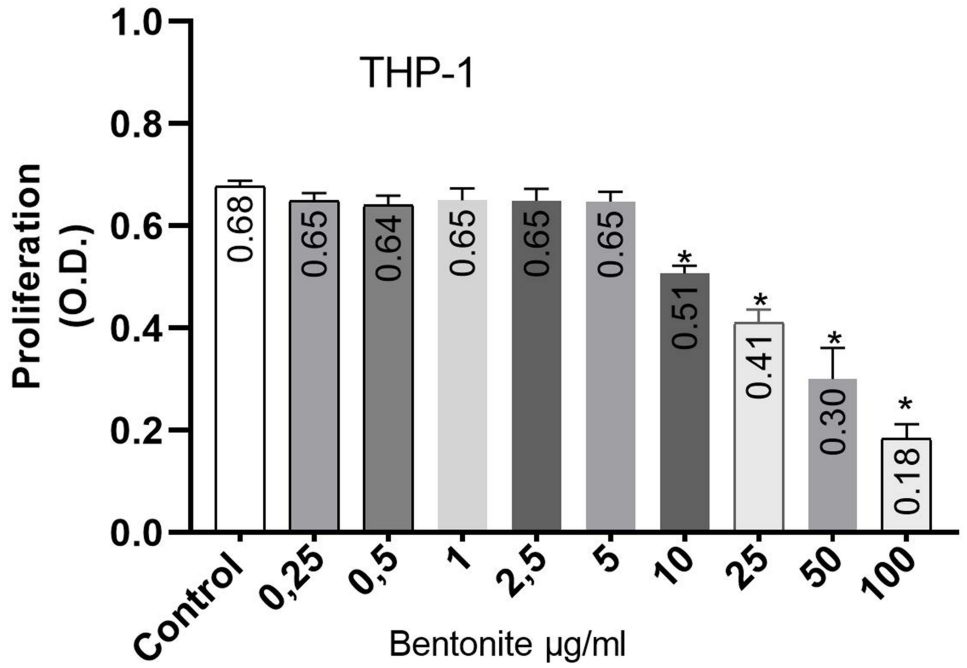

Figure 3 THP-1 cells proliferation test. Viability is expressed as absorbance value. *P < 0.05 indicates significant difference obtained as a result of comparison with the control group. The study was carried out in four replicates (n = 4).

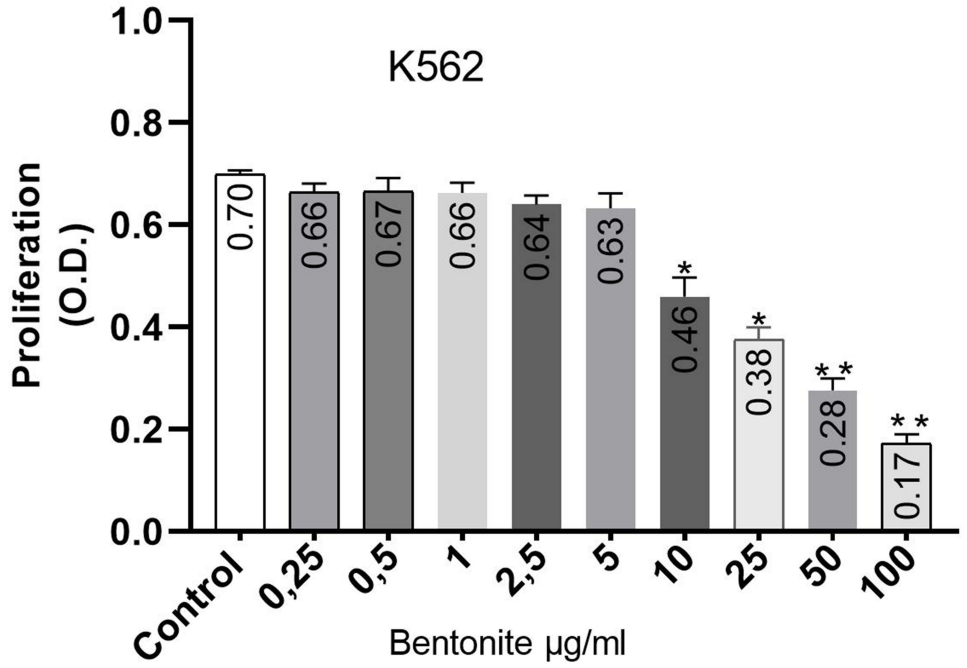

Figure 4 K562 cells proliferation test. Viability is expressed as absorbance value. *P < 0.05, **p < 0.001 indicates significant difference obtained as a result of comparison with the control group. The study was carried out in four replicates (n = 4).

the varying concentrations of AZA (1µM, 5µM, 10µM) and the combined groups (1µM AZA+10µg/mL BNT, 5µM AZA +10µg/mL BNT, 10µM AZA+10µg/mL BNT), and a group treated only with BNT (10µM) The results demonstrated that cell viability decreased and the inhibitory effect on cell proliferation increased with higher concentrations of AZA in

THP-1 cells. A significant difference was observed between the BNT-treated group and the control group. Furthermore, the combination of AZA and BNT resulted in a significant decrease in cell viability, indicating a strong anti-proliferative effect in the 1μM AZA+10μg/mL BNT, 5μM AZA+10μg/mL BNT, and 10μM AZA+10μg/mL BNT groups compared to that in the control group. Additionally, when the group treated with 1μM azacitidyine was compared to the group treated with 1μM AZA+10μg/mL BNT, a significant reduction in cell viability was observed, demonstrating the additive effect of the combination. In conclusion, the study revealed that the combination of AZA and BNT had a synergistic effect in inhibiting cell proliferation.(Figure 5).

In this study, as depicted in Figure 6, the cell viability in the K-562 cell line was observed to decrease considerably in the groups treated with 1μM, 5μM, and 10μM concentrations of AZA when compared to the control group. In addition, when AZA was combined with BNT, a significant anti-proliferative effect was observed in the 1μM AZA+10μg/mL BNT, 5μM AZA+10μg/mL BNT, and 10μM AZA+10μg/mL BNT groups compared to the control group. Furthermore, it was observed that the group treated with only 1μM AZA had a synergistic effect, with a significant decrease in cell viability compared to AZA alone. Additionally, when the 5μM AZA group was compared to the 5μM AZA+10μg/mL BNT combination group, there was a significant decrease in cell viability compared to AZA alone. It was found that in these groups, the antiproliferative effect of AZA was significantly enhanced with the addition of BNT.(Figure 6).

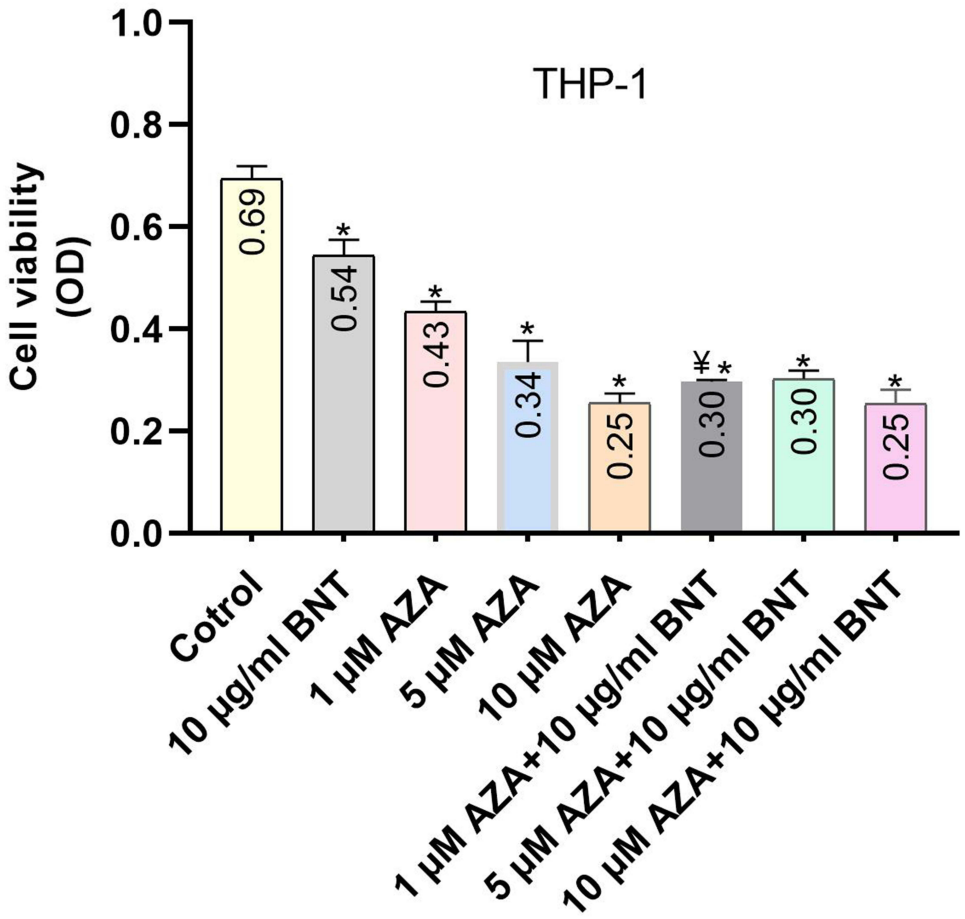

Figure 5 The impact of bentonite (BNT), azacytidine (AZA), and various combinations of these substances on the proliferation of THP-1 cells was examined. AZA was tested at concentrations of 1μM, 5μM, and 10μM, while BNT was tested at a concentration of 10μg/mL. Combinations of AZA and BNT were tested at 1μM AZA and 10μg/mL BNT, 5μM AZA and 10μg/mL BNT, and 10μM AZA and 10μg/mL BNT. The data points for AZA and BNT represent the mean ± standard deviation of the triplicate experiments. *P < 0.05, indicates a significant difference compared to the control group, and ¥P < 0.05, indicates significant difference compared to the 1μM AZA group.

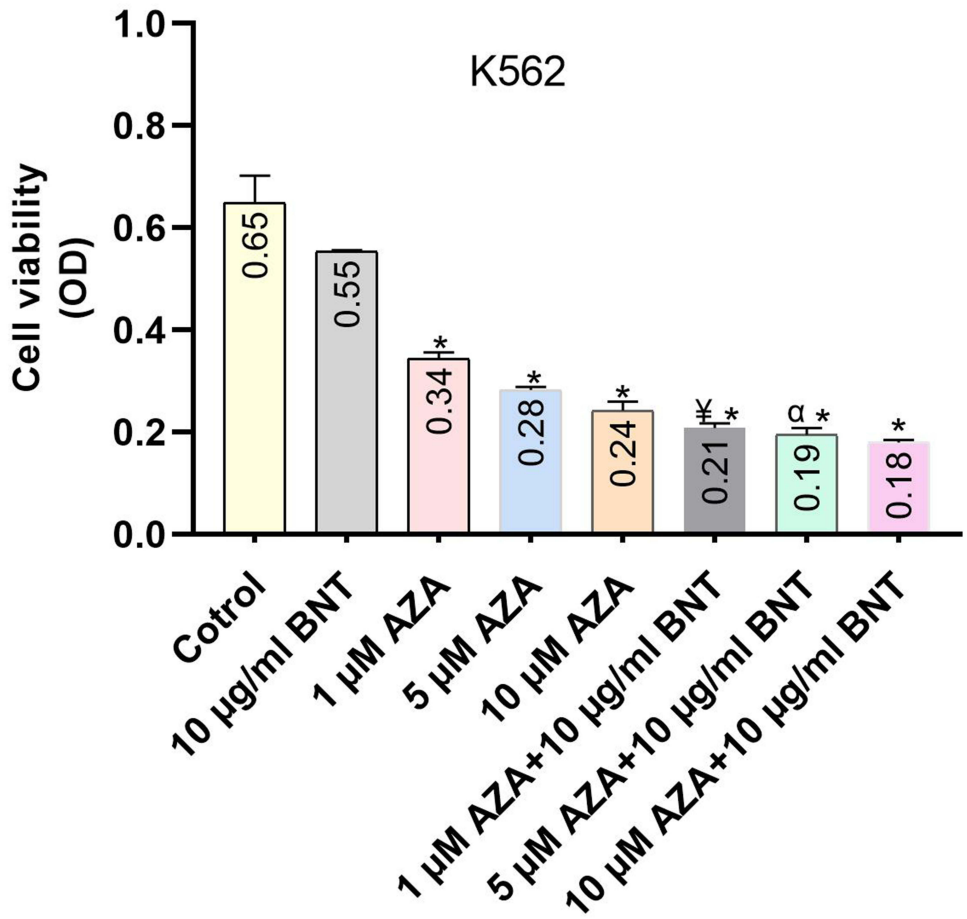

Figure 6 Effect of bentonite (BNT), azacitidine (AZA), BNT+AZA combinations on cell proliferation in K562 cells. AZA at concentrations of 1 µM, 5 µM, and 10 µM, as well as BNT at a concentration of 10 µg/mL, were applied in combination with AZA and BNT at various concentrations (1 µM AZA + 10 µg/mL BNT, 5 µM AZA + 10 µg/mL BNT, and 10 µM AZA + 10 µg/mL BNT). The mean ± standard deviation of the triplicate experiments for AZA and BNT are represented by the data points. The results indicate that there is a significant difference between the control group and the other groups, as indicated by the *P<0.05. Additionally, there is a significant difference between the 1 µM AZA group and the other groups, as indicated by the $^{¥}P < 0.05$ value, and significant difference between the 5 µM AZA group and the other groups, as indicated by the $^{α}P < 0.05$. The study was conducted with four replicates (n=4).

Internalization Test

In this study, the time-dependent cellular entry properties of the fluorescent agents, doxorubicin and doxorubicin-loaded BNT minerals, were investigated using flow cytometry. The study consisted of comparing the average fluorescence intensity of cells treated with DOX-loaded BNT and free Dox to that of the control group at 30 min, 4 h, and 24 h of incubation. The P3, P4, P5, P6, P7, and P8 gates in the analysis graph represent the percentage of cells internalising the fluorescent agent relative to the total cell population. Furthermore, the average fluorescence intensity of cells internalising the agent doxorubicin relative to cell numbers is illustrated in graphs at the 30th minute, 4th hour, and 24th hour intervals. Flow cytometry results revealed that in THP-1 cells, internalisation occurred at comparable rates in both the free doxorubicin and doxorubicin-loaded BNT groups at the 30th min. At the 4th hour of incubation, 93.7% of cells in the dox group and 73.4% of cells in the dox-BNT group internalized the agent. At the 24th hour of incubation, 94.7% of cells in the dox group and 91% of cells in the dox-BNT group internalized the agent (Figure 7).

In K562 cells, comparable rates of cell internalization were observed for free doxorubicin and doxorubicin-loaded BNT groups at 30 minutes, when compared to the control group. At the 4th hour of incubation, 87.3% of the cells in the dox group and 86.9% of the cells in the doxBNT group underwent dox internalization. At the 24th hour of incubation,

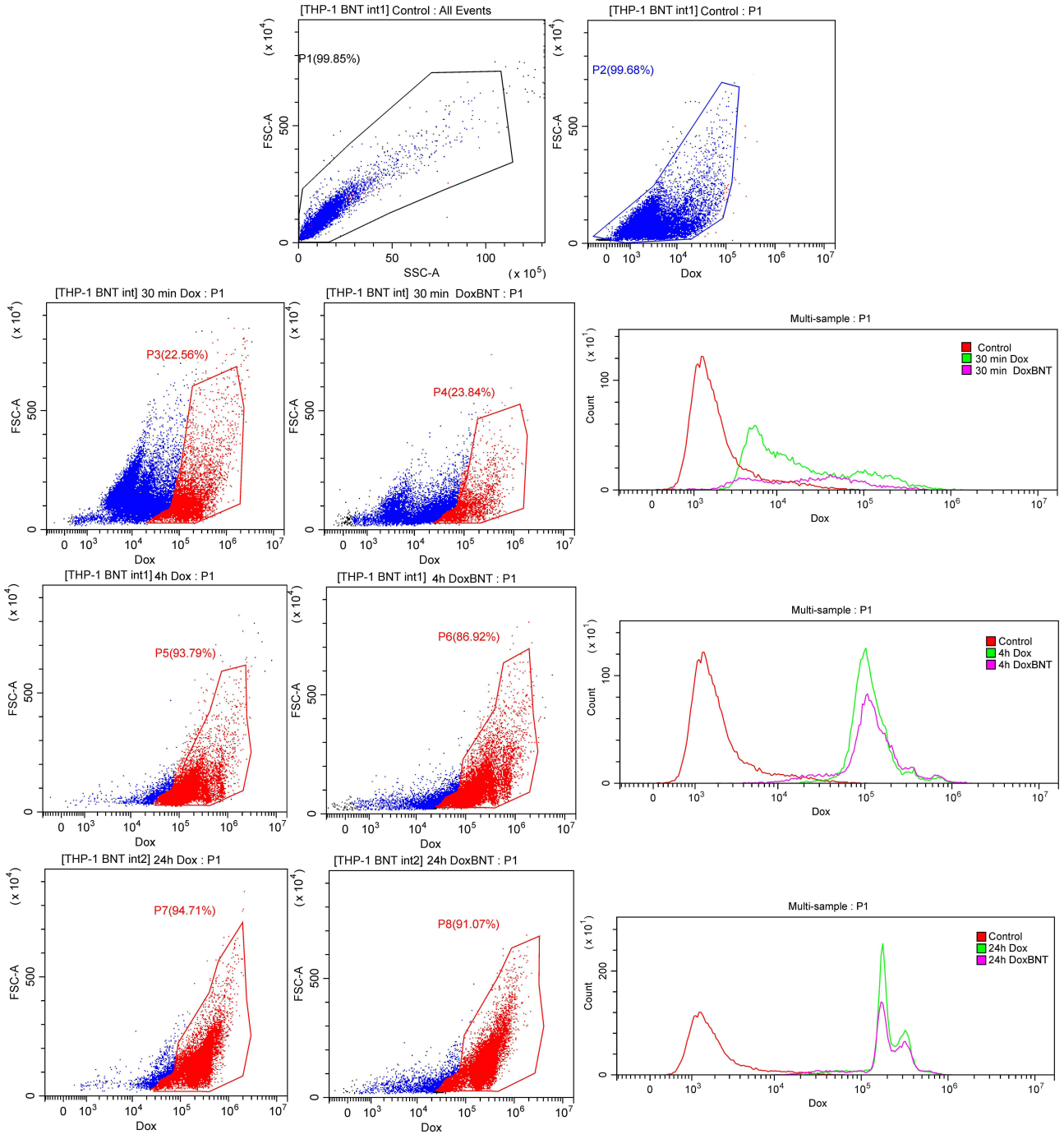

Figure 7 Flow cytometry cell internalization analysis of Dox and Dox loaded BNT in THP-1 cell line.

95.5% of the cells in the dox group and 86.8% of the cells in the dox-BNT group underwent dox internalization. (Figure 8).

Apoptosis Test

Following the application of AZA (10 µM), as well as BNT+AZA (10 µM AZA + 10 µg/mL BNT g/mL) and BNT (10 µg/mL) solutions to THP-1 and K562 cells, the induction of apoptosis was assessed via flow cytometry after staining with Annexin V-FITC and propidium iodide (PI). The results of the flow cytometry analysis are illustrated in Figures 9 and 10. The total percentage of cells in the lower and upper right quadrants in the analysis graph was determined as the percentage of

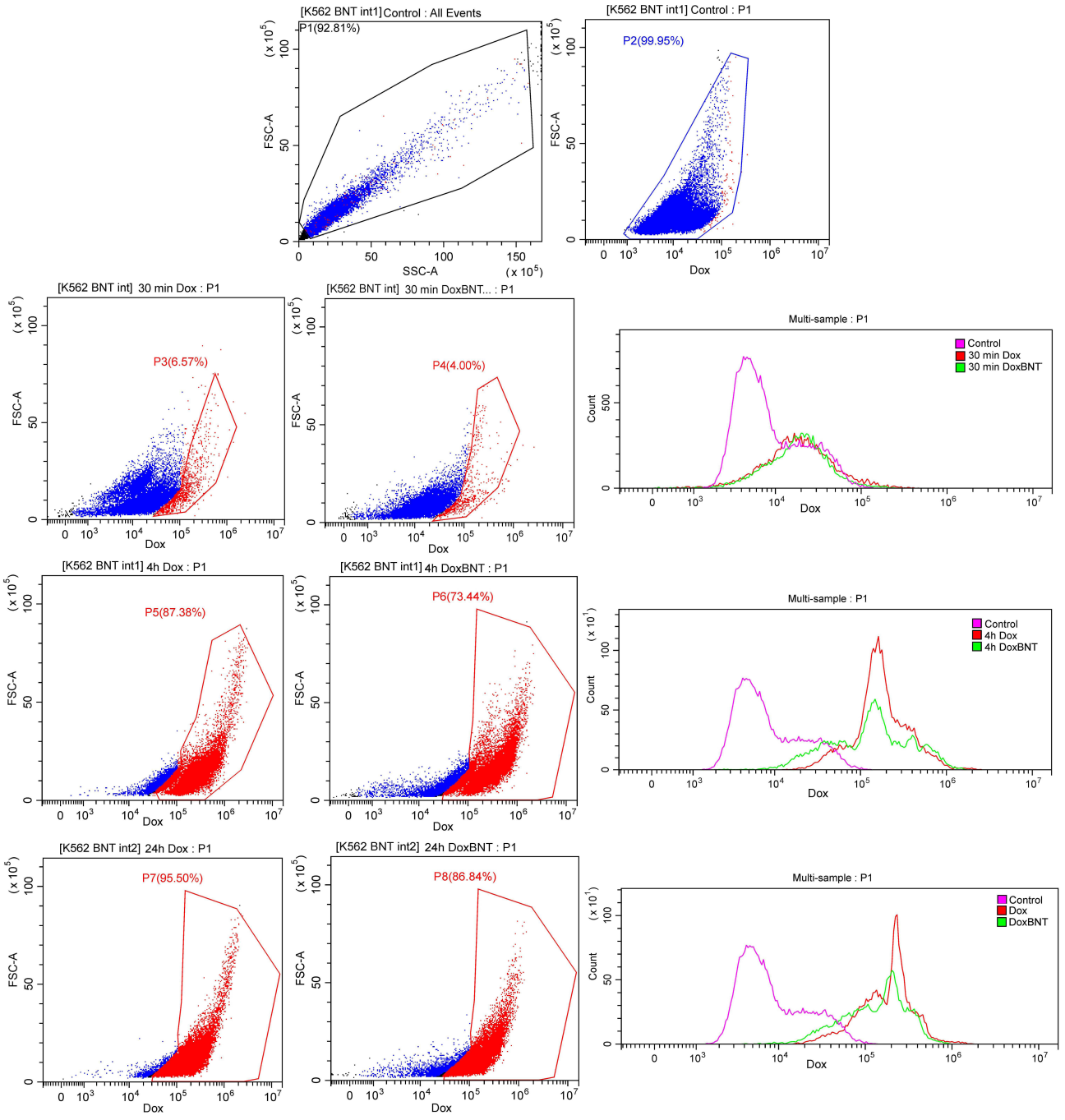

Figure 8 Flow cytometry cell internalization analysis of Dox and Dox loaded BNT in K562 cell line.

apoptotic cells. The analysis results are presented as percentages with bar graphs. After 24 h of application, the overall apoptosis rate (including early and late apoptosis) was 135% in the THP-1 AZA group, 290%, and 105% in the BNT group, respectively (Figure 9). In K562 cells, after 24 h of treatment, the overall apoptosis rates were 121%, 254%, and 131% in the AZA, BNT+AZA, and BNT groups, respectively (Figure 10). In the groups where the AZA+bentonite combination was applied to the THP-1 and K562 cell lines, the total apoptosis percentage significantly increased.

Ki-67 Expression

In this study, the expression of Ki-67 was evaluated using Western blotting in THP-1 and K562 cell lines. Specifically, the study assessed Ki-67 expression in BNT, AZA, and BNT+AZA groups. According to the protein expression data, no changes in Ki-67 expression were observed in with 10 µg/mL BNT or 1 µM AZA applied group in THP-1 cells. However, a decrease in Ki-67

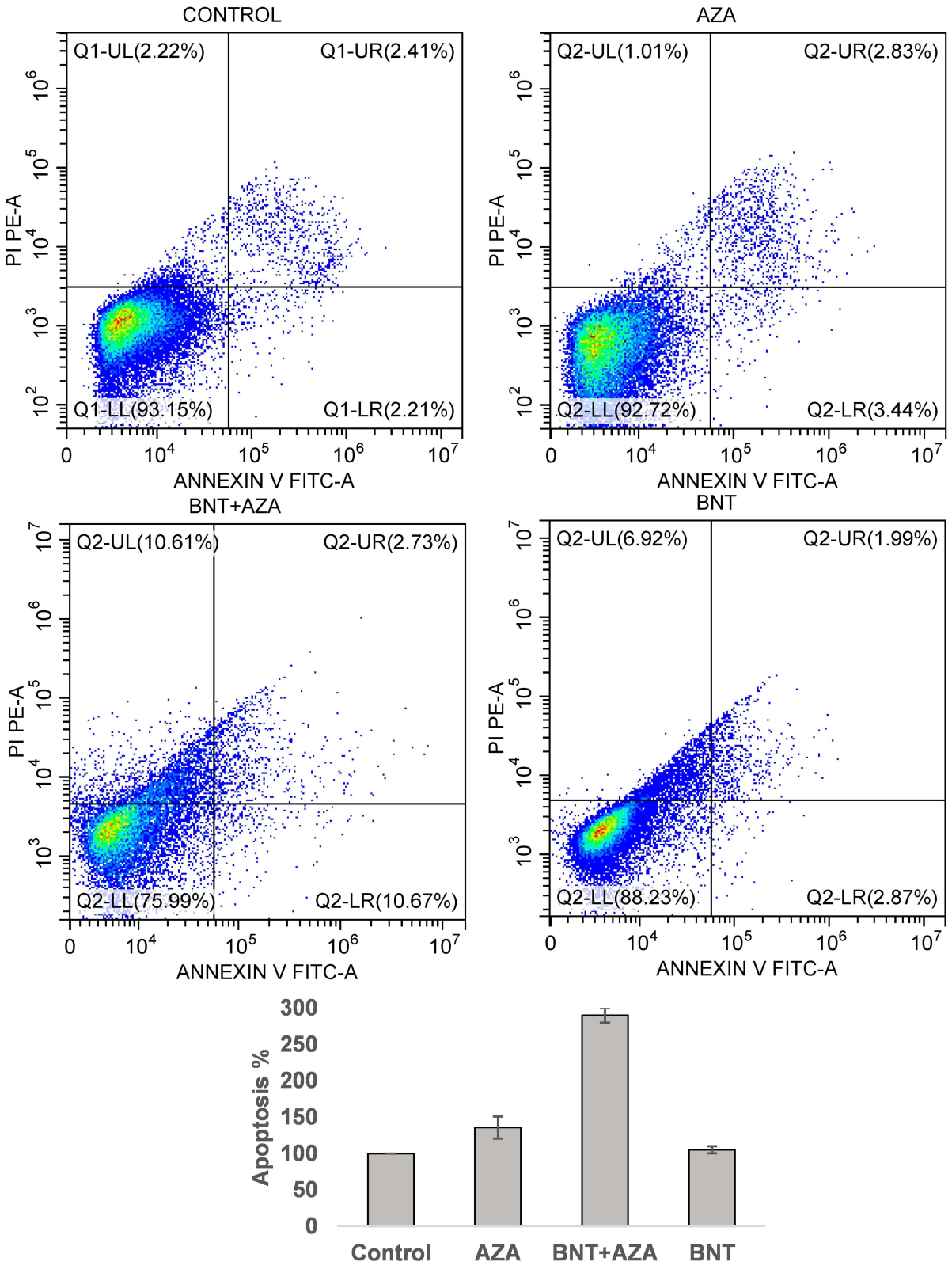

Figure 9 THP-1 cell line apoptosis assay. Cells were treated with AZA, BNT+AZA ant BNT for 24 h. Values are the means ± SD of three independent experiments.

expression was observed in the 5 and 10 μM AZA-treated groups. It is noteworthy that when the combination groups were compared to both the control group and the groups treated with BNT or AZA alone, a decrease in Ki-67 expression was observed (Figure 11).

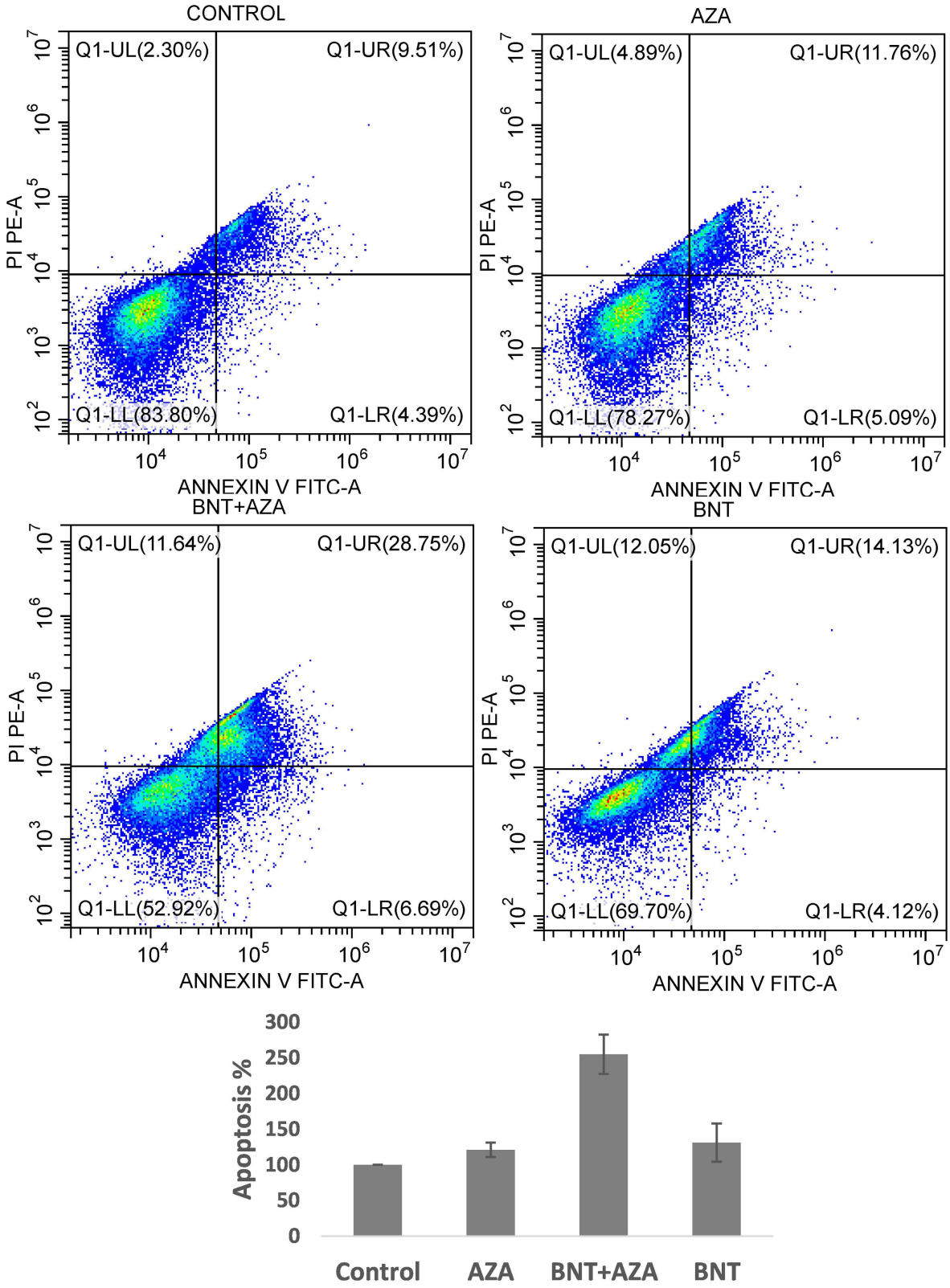

Figure 10 K562 cell line apoptosis assay. Cells were treated with AZA, BNT+AZA ant BNT for 24 h. Values are the means ± SD of three independent experiments.

In K562 cells, there was no noticeable change in the expression of Ki-67 in the group that received 10µg/mL µg/mL BNT and 1µM, 5µM, or 10µM µM AZA when compared to the control group. However, there was a decrease in Ki-67 expression in the combination groups of 5µM AZA+10µg/mL BNT and 10µM AZA+10µg/mL BNT compared to the control group (Figure 11).

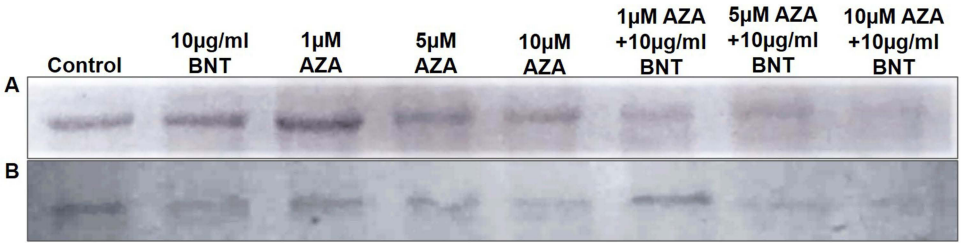

Figure 11 Western blot analysis of Ki-67 protein expression in THP-1 cells (**A**) and K562 cells (**B**). Protein expression levels are shown as band density on nitrocellulose membrane.

Abbreviations: CO^2, Carbon Dioxide; CCK-8, Cell Counting Kit-8; PBS, Phosphate Buffer Saline; SDS, Sodium Dodecyl Sulfate; HEPES, N-2-Hydroxyethylpiperazine-N-2-Ethanesulfonic Acid; EDTA, Ethylene Diamine Tetra Acetic Acid; NaCl, Sodium Chloride; SDS PAGE, Sodium Dodecyl Sulfate Polyacryl Gel Electrophoresis; ECL, Electrochemical Luminescence; MTT, Montmorillonite; BNT, Bentonite; AZA, Azacitidine; NP, Nanoparticle; HMA, Hypomethylating agent; Dox, Doxorubicin; DNMT, DNA methyltransferase; CDA, Cytidine deaminase.

Discussion

Cancer treatment requires swift and effective measures due to high mortality and morbidity rates. A major challenge is the specificity of treatments and side effects of chemotherapy, which lack smart system integration. Advanced therapies, such as monoclonal antibodies, enzyme pathway inhibitors, and CAR-T cells, aim for targeted treatment, while ongoing research focuses on drug carrier systems to enhance drug delivery to targets. Clay mineral particles have emerged as promising candidates for drug carrier NPs because of their efficacy in loading drugs and ensuring controlled release and targeted delivery to tumour sites. In addition to drug delivery, clay NPs exhibit antiproliferative effects, enhance cell-cell and extracellular matrix adhesion among cancer cells, and inhibit metastasis. They also offer therapeutic advantages for drugs with poor gastrointestinal absorption, improved solubility, bioavailability, controlled release, and protection from harsh environments such as stomach acids. Overall, clay NPs showed significant potential as drug carriers for cancer treatment.

The size and morphological characteristics of NP clays are crucial for their functional properties. It has been established that particles with size of 10–200 nm are beneficial during the transition phase, especially in terms of cellular permeability.[16] The BNT clay mineral that we utilised has been demonstrated to possess a size ranging from to 100–1000 nm. (Figure 1) The permeability of tissues other than tumour tissues can be reduced to <5 nm. The size range of the vascular space in tumour tissues is approximately 400–800 nm. This implies that large NPs are more likely to be enriched in the tumour environment and tissue and are less likely to pass into normal tissues. According to the flow cytometry results of our study, in the examination of the entry of the fluorescent agent Dox and dox-loaded BNT minerals into the cells using the flow cytometry technique, while there was no significant change in the in vitro internalisation profile at the 1st hour with the loading of Dox into the clay mineral, an increase in fluorescence intensity was observed at the 4th hour. At the 24th hour, the hydrophobic dye was internalised into the cells in all the groups (Figures 7–8). BNT NP, with their large surface area and cation exchange capacity, can more easily adhere to the cell membrane and be internalized through endocytosis. This feature is particularly important in applications targeting cancer cells, as it enables the drug to reach the target cells with high efficacy.

5-AZA has a relatively short half-life, which is achieved via hydrolysis or enzymatic deamination. Although the subcutaneous (SC) form is commonly used, the recently developed oral form is anticipated to become more widely utilised. The Tmax period for SC AZA is 0.5 hours, and its mean half-life after administration is 41 min. The mean elimination half-life of AZA and its metabolites was approximately 4 h after both intravenous and subcutaneous administration.[17] In a study assessing the plasma concentrations of oral AZA, it was observed that AZA was rapidly absorbed and reached an average Cmax within 1.5 hours after administration at doses of 200–300 mg. However, AZA concentrations in the blood could not be measured after the 6th hour.[18] The short plasma half-life of AZA may be considered a drawback in terms of its limited plasma stability and effectiveness in treating hypomethylating leukaemia cells. BNT can help protect healthy cells by providing minimal toxicity by slow controlled drug release and limits the systemic distribution of the drug, thus contributing to a reduction in side effects. This is especially advantageous in

clinical contexts like chemotherapy. Compared to other nanoparticle systems, bentonite is promising for clinical use due to its low cost, biocompatibility, and safety as a drug delivery system.

AZA is a chemotherapeutic agent and a cytosine analogue hypomethylating molecule. BNT can form electrostatic bonds with positively charged and negatively charged AZA molecules, and exchangeable cations can be exchanged with AZA to increase the interlayer space, which provides the ability to trap more molecules. This interaction also protects AZA enzymatic deamination. The positive charge of AZA is the main carrier mechanism of electrostatic interactions and attraction force binding between negatively charged BNT NP.[18,19] Furthermore, BNT-NP carriers can also exhibit a passive drug activity effect with increased permeability and accumulation in the cell. AZA showed a slow release profile with confinement in the intermediate layers and cation exchange. In the drug release test of the BNT-AZA combination, 50% was released in the first two hours, and almost 90% in the fourth hour, and it was detected in plasma until the eighth hour. (Figure 2) Additionally, it is important to note that the drug is not released explosively, which partially increases its effectiveness in target cells. The slow-release feature and absence of an explosive effect may result in a decrease in possible side effects. Combination applications may provide additional contributions in terms of increasing the adhesion-penetration and cytotoxicity of AZA to leukaemia cells and reducing the amount of drug used. Furthermore, the carrier molecule is natural, accessible, and inexpensive, which also provides an economic advantage.

BNT NPs exhibit varying effects on cells, demonstrating both cytotoxicity and cytoprotective properties. In research conducted on human lymphoblast cells, lysis of the cell surface and increased oxidative stress were identified as the primary pathways of cytotoxicity. Additionally, a study on two distinct clays revealed genotoxicity in cellular RNA as a notable pathway.[20] The impact of BNT on cells is dependent on its concentration and may be influenced by the physiochemical characteristics of clay minerals and the duration of exposure. BNT displayed a dose-dependent effect on THP-1 and K562 cell lines after 48 h of incubation, with IC50 obtained at doses of 25–50 µg/mL in both cell cultures. The effects of BNT on different cell types vary depending on the dose and duration of exposure. For instance, colon cancer cell lines exposed to 20 µg/mL of organic-modified BNT for 24 and 48 h revealed morphological changes, matrix damage, and inner membrane damage. The same product exhibits distinct effects on different cell lines at varying doses and time intervals.[21] BNT has distinct effects on the proliferation of U251 and SKLU-1 cells. It induced growth inhibition in the presence of U251 cells and stimulated cell growth in the presence of SKLU-1 cells. BNT demonstrates varying effects on different cell types. It exhibited antiproliferative properties in both the myeloid cell lines examined.[22] From an alternative viewpoint, it is plausible that distinct clay NPs may have varying impacts on the same cell line at different concentrations or even have no effect at all. In the case of K550 cell culture, BNT appeared to inhibit cell proliferation after a 48-hour incubation period when the concentration exceeded 0.05 mg/mL, whereas zeolite demonstrated inhibitory effects at 10 and 5 mg/mL. However, no such effect was observed with sepiolite. The influence of the different physicochemical properties of various clays is also noteworthy.[23] The choice of clay, its dosage, and the resulting impact on the target cells are all factors of significance.

A study conducted by our research team revealed that there was no notable toxicity observed in THP-1 and K562 cells when treated with clay minerals at low concentrations, including 0.25 µg/mL, 0.5, 1, 2.5, and 5 µg/mL ($p > 0.05$) (Figures 3 and 4). However, at a concentration of 10 µg/mL, there was an increased antiproliferative effect, which was more pronounced at doses of 25, 50, and 100 µg/mL. At 100 µg/mL, both K-562 and THP-1 cells exhibited a significant decrease in cell viability ($p < 0.05$). In the analysis of apoptosis, which was assessed by flow cytometry with annexin, it was observed that after 24 h of treatment in the THP-1 group, the total apoptosis rate (early and late apoptosis) was 135% in the AZA (10 µM) group, 290% in the BNT + AZA (10 µM AZA + 10 µg/mL BNT g/mL) group, and 105% in the BNT (10 µg/mL) group. The total apoptosis rates of K562 cells were 121%, 254%, and 131% in the AZA, BNT+AZA, and BNT groups, respectively, after 24 h of treatment. (Figure 10). In the experimental groups in which the combination of AZA and bentonite was applied to THP-1 and K562 cell lines, there was a significant increase in the total apoptosis percentage. Furthermore, we observed a decrease in the Ki67 proliferation index when the combination was used, particularly in BNT-AZA studies (Figure 11). The decrease in cell viability at high concentrations of clay minerals may be attributed to the membrane damaging effects of clay mineral particles, resulting in necrotic cell death rather than apoptosis. It has been reported that high amounts of clay minerals can cause liposome lysis because of the direct interaction between the cell and particles, regardless of their composition, as a result of environmental effects such as

cation exchange and adsorption capacity. In all three analysis techniques, a more effective response was obtained with the combined use of BNT-AZA.

In vitro cytotoxicity assays were performed to evaluate the anticancer potential of BNT-AZA particles using THP-1 and K562 cell lines. The cytotoxicity of pure BNT and AZA-loaded clay minerals was tested in K562 and THP-1 cells (Figures 5 and 6). BNT (10 µM) was used in both cell cultures, resulting in a 22% decrease in cell viability for THP-1 cells and a 16% decrease in K562 cell viability. The results showed a significant decrease in cell viability compared to that in the control group. In K562 cells, 1, 5, and 10 µM AZA in combination with 10 µg/mL BNT reduced cell viability by 39%, 33%, and 25%, respectively. The addition of BNT to all three doses of AZA resulted in cell death. A similar outcome was evident when BNT was combined with AZA at different concentrations; 1µM AZA+10µg/mL BNT reduced cell viability by 32%, while 5µM AZA+10µg/mL BNT led to a decrease of 12%. Apoptosis was more pronounced in K562 cells than in THP-1 cells, likely due to the distinct characteristics of each cell type and the atypical, resistant nature of the K562 cell line compared to THP-1 cells. The combination of AZA and BNT displays divergent pharmacodynamic and pharmacokinetic properties in cellular terms. The observation that the addition of 1, 5, and 10 µM AZA to 10 µg/mL BNT did not result in significant changes in the treatment response suggests that it may be related to cellular saturation in response to chemotherapy. The finding that the cell survival response obtained with 10 µM AZA was more effectively achieved with 1 µM AZA+10 µg/mL BNT suggests that it may be possible to achieve the same effect at lower drug doses, potentially resulting in cost savings in terms of pharmacoeconomics. Beyond electrostatic interaction, controlled release, and cellular pore interaction, other potential mechanisms underlying the efficacy of the BNT-AZA combination include intracellular pH responsiveness, increased cytotoxic effect, nanoparticle stability, and enhanced intracellular bioavailability. Evidence suggests that BNT enhances AZA's effectiveness in the acidic tumor microenvironment. Since AZA is sensitive to intracellular pH, pH-responsive carriers like bentonite activate AZA's cytotoxic effect at a higher level specifically in target tumor cells. The structural stability of BNT allows AZA to remain inside the cell longer, improving its bioavailability. This feature optimizes AZA's effectiveness at the cellular level and increases cell death rates throughout the treatment period.[24,25] These combined mechanisms make BNT not only an efficient carrier for targeted drug delivery but also a transformative platform in enhancing the impact of chemotherapeutics like AZA in leukemia treatment.

Comparison of the BNT-AZA combination with other drug delivery systems is valuable in terms of contextualising the effectiveness of the proposed treatment strategy. Clay-based carriers, such as bentonite nanoparticles, have been hypothesised to offer several advantages over other nanoparticle delivery systems. Owing to its pH sensitivity, porous structure, large surface area, cation exchange capacity, and biocompatibility, the combination of bentonite with drugs such as AZA has the potential to provide targeted controlled release. However, some features of other targeted therapies have not yet been elucidated, including the absence of specific targeting (ie no receptor binding) and the issue of distribution in the biological system. Compared with alternative drug carriers, bentonite is considered a suitable option for controlled drug release because of its stability and biocompatibility.[26] Carrier systems, such as polymeric nanoparticles (eg, PLGA and PEG), may degrade within the body because of their limited biocompatibility, whereas BNT can provide a more rapid and efficient release.[27] Liposomes and solid lipid nanoparticle carriers readily integrate into cell membranes and offer higher bioavailability than bentonite. However, the stability and low toxicity of bentonite confers significant advantages.[28] Silica-based nanoparticles enable controlled release through their porous structures, whereas BNT offers a more rapid release with lower toxicity, while maintaining biocompatibility.[29,30] This appears to be more advantageous for long-term use. However, these limitations can be overcome by incorporating polymers into BNT. Given these characteristics, this approach shows significant potential to enhance the efficacy of current treatments and reduce side effects. With its low cost, large surface area, and biocompatibility, bentonite stands out as a strong carrier system for controlled drug release. These properties make bentonite more appealing than other carriers in treatments where cost and biocompatibility are critical.

Our study has some limitations. Among these, the use of NP polymers (such as PLGA, PEG) integrated with BNT was not attempted, as we designed our study without polymer conjugation. The use of polymers could yield a more effective, more antiproliferative and cytotoxic, and prolonged-release profile. We recorded the drug release profile up to the 8th hour; however, the plateau phase in the release graph indicates that the process may continue. Employing the LDH assay to

measure potential damage to cell membrane integrity could have made our study results more impactful, conclusive, and consistent. If we had included normal myeloid and lymphoid cell lines, we could have obtained information on whether cytotoxicity occurs in these cells and, if so, at which doses. Lastly, in myeloid leukemia cells, the TUNEL Assay could have been used to measure DNA damage, and PCR could have been employed to determine effects on gene expression levels. In the future, the incorporation of biocompatible polymers (such as PLGA or PEG) into BNT nanoparticles could offer more controlled and prolonged drug release. Such polymer conjugation may contribute to effective drug accumulation in the target tissue while reducing systemic side effects, thus providing a safer treatment profile. Additionally, the use of BNT as a multidrug carrier could create new opportunities for combining different therapeutic approaches, such as chemotherapy and immunotherapy. Bentonite's ability to carry multiple drugs simultaneously holds the potential to produce synergistic therapeutic effects, making this combination especially promising in cancer treatment. Furthermore, targeting specific tumour cells through surface modifications of bentonite nanoparticles could be crucial for enhancing therapeutic efficacy. Strengthening the targeting capacity of nanoparticles by adding ligands or antibodies that can bind to specific receptors on the cell surface is feasible. Therefore, in vivo studies are of high priority and significance. Such studies enable a detailed examination of the biocompatibility and potential side effects of nanoparticles and represent a crucial step toward clinical application. Additionally, it is essential to understand how bentonite affects cellular mechanisms, particularly in terms of gene expression changes and cellular pathways. These mechanistic studies will aid in gaining a better understanding of the effectiveness of the drug on target cells and contribute to the development of therapeutic strategies. Finally, pharmacokinetic analyses investigating the bioavailability and distribution of the drug carried by bentonite are crucial for assessing the clinical efficacy of this carrier system. These results suggest that bentonite-based drug delivery systems may play an important role in more effective, safer, and targeted treatment approaches in the future.

Conclusion

Our study aimed to achieve more effective responses in cancer treatment with targeted therapy and lower side effects. We found that the AZA-BNT combination therapy enhanced cell cytotoxicity and proliferation response compared to pure AZA. Notably, combining AZA with lower doses of BNT produced the same response as high doses of AZA, suggesting potential pharmacoeconomic and side effect advantages for future applications. Another benefit of BNT is its ability to facilitate the slow release and delayed metabolism of AZA, indicating increased treatment efficacy. We believe that clay NPs are promising in this field and that further studies will illuminate their potential. In vitro studies provide valuable insights into nanoparticle behaviour, cellular uptake, and drug delivery mechanisms in controlled environments. However, the complexity of biological systems necessitates in vivo research to assess how these nanoparticles interact within the full scope of an organism, including biodistribution, toxicity, immune response, and therapeutic efficacy in targeting tumours. Recent advancements in nanoparticle design, such as pH-sensitive and surface-modified nanoparticles, have exhibited promising results in preliminary studies; however, rigorous in vivo validation is essential to translate these findings into clinically relevant outcomes. The integration of in vitro, in vivo approaches and pharmacokinetic analyses will not only strengthen the evidence for nanoparticle efficacy but also expedite the development of novel, targeted, and effective cancer therapies that can offer improved outcomes for patients.

Acknowledgments

Mustafa Duran and Elif Kaga contributed equally to this work. They both helped in preparing the manuscript. They both read and approved the final manuscript.

Funding

This study was supported by the Afyonkarahisar Health Sciences University, Scientific Research Project Unit (BAP) grant 23.GENEL.011.

Disclosure

The author(s) report no conflicts of interest in this work.

References

1. Mitchell MJ, Billingsley MM, Haley RM, Wechsler ME, Peppas NA, Langer R. Engineering precision nanoparticles for drug delivery. *Nat Rev*. 2021(20):101–124.
2. Yang JH, Lee JH, Ryu HJ, Elzatahry AA, Alothman ZA, Choy JH. Drug–clay nanohybrids as sustained delivery systems. *Appl Clay Sci*. 2016;130:20–32. doi:10.1016/j.clay.2016.01.021
3. Aguzzi C, Cerezo P, Viseras C, Caramella C. Use of clays as drug delivery systems: possibilities and limitations. *Appl Clay Sci*. 2007;36 (1–3):22–36. doi:10.1016/j.clay.2006.06.015
4. Khatoon N, Chu MQ, Zhou CH. Nanoclay-based drug delivery systems and their therapeutic potentials. *J Mater Chem B*. 2020;8:7335–7351. doi:10.1039/D0TB01031F
5. Rojtanatanya S, Pongjanyakul T. Propranolol–magnesium aluminum silicate complex dispersions and particles: characterization and factors influencing drug release. *Int J Pharm*. 2010;383:106–115. doi:10.1016/j.ijpharm.2009.09.016
6. Bates DO, Hillman NJ, Williams B, Neal CR, Pocock TM. Regulation of microvascular permeability by vascular endothelial growth factors. *J Anat*. 2002;200(6):581–597. doi:10.1046/j.1469-7580.2002.00066.x
7. Swartz MA, Mark E FleuryInstitute of Bioengineering (2007) Interstitial flow and its effects in soft tissues.
8. Attia MF, Anton N, Wallyn J, Omran Z, Vandamme TF An overview of active and passive targeting strategies to improve the nanocarriers efficiency to tumour sites; 2019.
9. Peer D, Karp JM, Hong S, et al. Nanocarriers as an emerging platform for cancer therapy. *Nat Nanotechnol*. 2007;2(12):751–760. doi:10.1038/nnano.2007.387
10. Kamaly N, Xiao Z, Valencia PM, Radovic-Moreno AF, Farokhzad OC. Targeted polymeric therapeutic nanoparticles: design, development and clinical translation. *Chem Soc Rev*. 2012;41(7):2971–3010. doi:10.1039/c2cs15344k
11. Byrne JD, Betancourt T, Brannon-Peppas L. Active targeting schemes for nanoparticle systems in cancer therapeutics. *Adv Drug Deliv Rev*. 2008;60 (15):1615–1626. doi:10.1016/j.addr.2008.08.005
12. Patra JK, Das G, Fraceto LF, et al. Nano based drug delivery systems: recent developments and future prospects. *J Nanobiotechnol*. 2018;16:71. doi:10.1186/s12951-018-0392-8
13. Kaushik N, Borkar SB, Nandanwar SK, et al. Nanocarrier cancer therapeutics with functional stimuli-responsive mechanisms. *J Nanobiotechnol*. 2022;20:152. doi:10.1186/s12951-022-01364-2
14. Dombret H, Seymour JF, Butrym A, et al. International Phase 3 study of azacitidine vs conventional care regimens in older patients with newly diagnosed AML with >30% blasts. *Blood*. 2015;126(3):291–299. doi:10.1182/blood-2015-01-621664
15. Garcia-Manero G, Döhner H, Wei AH, et al. Oral Azacitidine (CC-486) for the Treatment of Myeloid Malignancies. *Clin Lymphoma Myeloma Leukemia*. 2022;22(4):236–250. doi:10.1016/j.clml.2021.09.021
16. Poon W, Kingston BR, Ouyang B, Ngo W, Chan WCW. A framework for designing delivery systems. *Nat Nanotechnol*. 2020;15(10):819–829. PMID: 32895522. doi:10.1038/s41565-020-0759-5
17. Shen Y, Zhang Z, Wang Y. Controlled release of anticancer drugs using porous clay nanoparticles: enhancing stability and therapeutic efficacy. *J Drug Deliv Sci Technol*. 2021;60:101984. doi:10.1016/j.jddst.2021.101984
18. National Center for Biotechnology Information. PubChem Compound Summary for CID 9444, Azacitidine; 2024. Availabe from: https://pubchem.ncbi.nlm.nih.gov/compound/Azacitidine. Accessed August 5, 2024
19. Laille E, Shi T, Garcia-Manero G, et al. Pharmacokinetics and pharmacodynamics with extended dosing of CC-486 in patients with hematologic malignancies. *PLoS One*. 2015;10(8):e0135520. doi:10.1371/journal.pone.0135520
20. Rius M, Stresemann C, Keller D, et al. Human concentrative nucleoside transporter 1-mediated uptake of 5-azacytidine enhances DNA demethylation. *Mol Cancer Ther*. 2009;8(1):225–231. doi:10.1158/1535-7163.MCT-08-0743
21. Zhang M, Li X, Lu Y, Fang X, Chen Q, Xing M. Studying the genotoxic effects induced by two kinds of bentonite particles on human B lymphoblast cells in vitro. *Mutat Res*. 2011;720:62–66. doi:10.1016/j.mrgentox.2010.12.009
22. Maisanaba S, Gutiérrez-Praena D, Pichardo S, J MF, Jordá M. Toxic effects of a modified montmorillonite clay on the human intestinal cell line Caco-2. *J appl toxicol*. 2014;34:714–725. doi:10.1002/jat.2945
23. Nemati Shamsabad F, Salehi MH, Shams J, Ghazanfari T. Cytotoxicity of Bentonite, Zeolite, and Sepiolite Clay Minerals on Peripheral Blood Mononuclear Cells. *Immunoregulation*. 2023;5(2):121–130. doi:10.32598/IMMUNOREGULATION.5.2.6
24. Liu X, Wu Q, Feng L. pH-responsive drug delivery systems in cancer therapy: nanoparticle-mediated cytotoxicity in acidic tumor environments. *Adv Drug Deliv Rev*. 2019;141:82–101. doi:10.1016/j.addr.2019.04.009
25. Zhang L, Chan JM, Wang AZ. Stability of nanoparticles in biological media: challenges and strategies for drug delivery applications. *Nano Today*. 2018;20:73–91. doi:10.1016/j.nantod.2018.02.006
26. Wang J, Li X, Zhou H. Influence of nanoparticle surface charge on cellular uptake and targeted drug delivery in cancer therapy. *Nano Res*. 2020;13 (5):1369–1381. doi:10.1007/s12274-020-2820-1
27. Jang JH, Jeong SH, Lee YB. Preparation and in vitro/in vivo characterization of polymeric nanoparticles containing methotrexate to improve lymphatic delivery. *Int J Mol Sci*. 2019;20(13):3312. doi:10.3390/ijms20133312
28. Sharma H, Mondal S. Functionalized graphene oxide for chemotherapeutic drug delivery and cancer treatment: a promising material in nanomedicine. International. *J Molec Scie*. 2020;21(17):6280. doi:10.3390/ijms21176280
29. Li Y, Deng G, Hu X, et al. Recent advances in mesoporous silica nanoparticle-based targeted drug-delivery systems for cancer therapy. *Nanomedicine*. 2022;17(18):1253–1279. doi:10.2217/nnm-2022-0023
30. Geh S, Yücel R, Duffin R, et al. Cellular uptake and cytotoxic potential of respirable bentonite particles with different quartz contents and chemical modifications in human lung fibroblasts. *Arch Toxicol*. 2006;80(2):98–106. doi:10.1007/s00204-005-0013-9